Virology Journal

RESEARCH

Open Access

KCNE4 is a crucial host factor for Orf virus infection by mediating viral entry

Jiayuan Sun[1†], Yige Ding[1†], Qian Zhou[1], Peter Kalds[2], Jianlin Han[2], Keshan Zhang[3], Yinghui Wei[1,4,5], Weiwei Wu[6], Xiaolong Wang[1,4,5*] and Wenxin Zheng[6*]

Abstract

The orf virus (ORFV) poses a serious threat to the health of domestic small ruminants (i.e., sheep and goats) and humans on a global scale, causing around $150 million in annual losses to livestock industry. However, the host factors involved in ORFV infection and replication are still elusive. In this study, we compared the RNA-seq profiles of ORFV-infected or non-infected sheep testicular interstitial cells (STICs) and identified a novel host gene, *potassium voltage-gated channel subfamily E member 4* (*KCNE4*), as a key host factor involved in the ORFV infection. Both RNA-seq data and RT-qPCR assay revealed a significant increase in the expression of *KCNE4* in the infected STICs from 9 to 48 h post infection (hpi). On the other hand, the RT-qPCR assay detected a decrease in ORFV copy number in both the STICs transfected by *KCNE4* siRNA and the *KCNE4* knockout (KO) HeLa cells after the ORFV infection, together with a reduced fluorescence ratio of ORFV-GFP in the KO HeLa cells at 24 hpi, indicating *KCNE4* to be critical for the ORFV infection. Furthermore, the attachment and internalization assays showed decreased ORFV attachment, internalization, replication, and release by the KO HeLa cells, demonstrating a potential inhibition of ORFV entry into the cells by *KCNE4*. Pretreatment with the *KCNE4* inhibitors such as quinidine and fluoxetine significantly repressed the ORFV infection. All our findings reveal *KCNE4* as a novel host regulator of the ORFV entry and replication, shedding new insight into the interactive mechanism of ORFV infection. The study also highlights the K^+ channels as possible druggable targets to impede viral infection and disease.

Keywords Orf virus, RNA-seq, *KCNE4*, Viral entry, Inhibitor

Introduction

Ecthyma contagiosum is an acute contagious zoonotic disease caused by the orf virus (ORFV). ORFV is a member of the *Parapoxvirus* genus in the *Poxviridae* family. ORFV primarily infects domestic sheep and goats along with other wild small ruminants, and spreads to humans through direct contact with infected animals [1]. Accumulated evidence has revealed that the range of infected hosts of ORFV continues to expand [2]. ORFV mainly causes proliferative skin lesions around the lips, nostrils, and oral surfaces, resulting in a significant morbidity [3]. Although there is accumulated evidence regarding the virulence factors of ORFV, the interactive mechanism between ORFV and the hosts is poorly investigated [4,

†Jiayuan Sun and Yige Ding contributed equally to this work.

*Correspondence:
Xiaolong Wang
xiaolongwang@nwafu.edu.cn
Wenxin Zheng
zwx2020@126.com
[1]International Joint Agriculture Research Center for Animal Bio-breeding, Ministry of Agriculture and Rural Affairs, College of Animal Science and Technology, Northwest A&F University, Yangling 712100, China
[2]Yazhouwan National Laboratory, Sanya 572024, China
[3]Guangdong Provincial Key Laboratory of Animal Molecular Design and Precise Breeding, School of Life Science and Engineering, Foshan University, Foshan 528225, China
[4]Key Laboratory of Livestock Biology, Northwest A&F University, Yangling 712100, China
[5]School of Future Technology on Bio-breeding, Northwest A&F University, Yangling 712100, China
[6]Xinjiang Academy of Animal Sciences, Urumqi, Xinjiang 830011, China

5]. Considering that ORFV poses a serious threat to the sheep and goat industry as well as human health, it is urgent to dissect the interaction between ORFV and the hosts.

Ion channels are mainly located in the cytoplasmic membrane and subcellular organelles, and regulate intracellular and extracellular ion homeostasis [6, 7]. Various viruses have been found to be modulated by the ion channels. For instance, Cav1.2 has been revealed as a sialylated host cell surface receptor that binds haemagglutinin (HA) and is critical for influenza virus (IAV) entry [8]. Furthermore, bunyavirus (BUNV) traffics through endosomes that contain high K^+ to facilitate BUNV infection [9]. In addition, the Na^+ channel opener SDZ-201,106 or protein kinase C (PKC) inhibitor can reduce IAV replication [10].

Voltage-gated potassium ion channels (Kv) can control repolarization, they play an important role in returning the depolarized cell to a resting state, and they are also involved in the apoptosis process and the immune system [11, 12]. *Potassium voltage-gated channel subfamily E member 4* (*KCNE4*) is the 4th member of the KCNE Kv channel regulatory subunit family. *KCNE4* interacts with the Kv1.3 channel and acts as a dominant negative regulatory subunit to enhance inactivation and induce intracellular retention of Kv1.3 [13, 14]. Although previous studies have shown the physiological and pathological roles of *KCNE4* [6], the interactive mechanism between the *KCNE4* gene and ORFV infectious cycle remains unclear.

This study aims to explore the key host factors involved in the ORFV infection (Fig. 1). Since testicular interstitial cells (TICs) are determined as the ideal cell model for studying the ORFV infection, we therefore established the sheep TICs (STICs) for this investigation. By performing RNA-seq in infected and non-infected STICs, we identified considerable unreported host factors involved in the ORFV replication. Specifically, the *KCNE4* gene was found to be significantly upregulated in the ORFV-infected STICs. Subsequently, knocking down the *KCNE4* gene in the STICs and knocking out (KO) the *KCNE4* gene in HeLa cells significantly inhibited the ORFV infection. In addition, we found that *KCNE4* plays a critical role in ORFV entry into the *KCNE4* KO HeLa cells and the K^+ channel inhibitors such as quinidine or fluoxetine were able to effectively inhibit the ORFV infection. Taken together, these results indicate that *KCNE4* is an important host gene for the ORFV infection, which provides a better understanding of the ORFV-host interface and highlights the K^+ channels as potential druggable anti-viral targets.

Results

RNA-seq of ORFV-infected STICs

To investigate whether STICs are sensitive to ORFV, STICs were infected with ORFV at different multiplicity

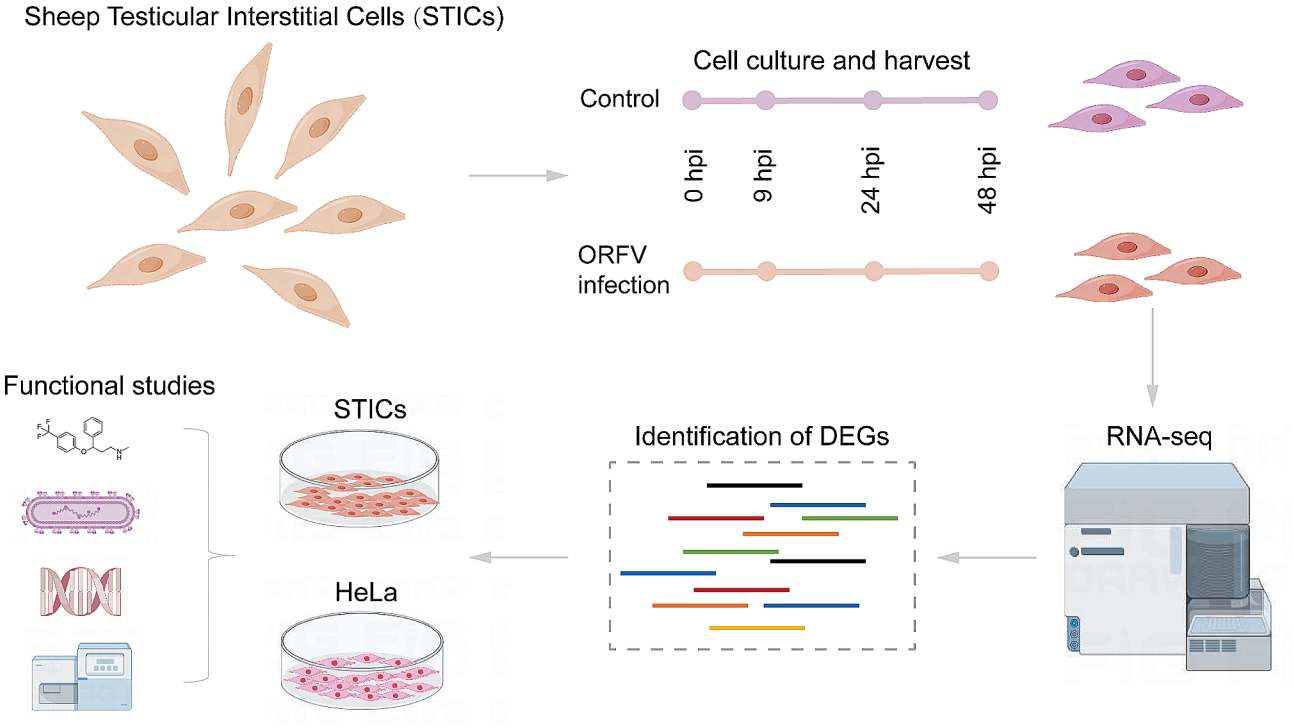

Fig. 1 Schematic illustration of the experimental workflow. The RNA-seq was applied to obtain comprehensive visualization of transcriptional profiles in the STICs throughout the ORFV infection, and the output data were used for integrative analyses and verified by multiple experiments

of infection (MOIs) and evaluated at 24-, 48-, and 72-hours post infection (hpi). We found that the ORFV-infected STICs exhibited obvious cytopathic effect (CPE) phenotypes such as wrinkling, shedding, and rounding (Fig. 2A). Subsequently, the reverse transcription quantitative PCR (RT-qPCR) assay detected an increased transcription of ORFV in the ORFV-infected STICS, forming an 'S'-shaped curve (Fig. 2B). Collectively, these results confirm that STICs can serve as a cell model for monitoring the ORFV infection.

To explore the molecular mechanism between the ORFV infection and STICs, we used an RNA-seq assay to quantify the transcriptomic changes in the cellular samples collected at 9, 24, and 48 hpi following the ORFV infection of the STICs at an MOI of 1. It was shown that the total numbers of differentially expressed genes (DEGs) between the ORFV-infected and non-infected STICs at 9, 24, and 48 hpi were 4,806 (2,397 upregulated and 2,409 downregulated), 4,437 (2,313 upregulated and 2,124 downregulated), and 11,487 (6,260 upregulated and 5,227 downregulated), respectively. The enrichment analysis of gene ontology (GO) "biological process" annotations was performed to classify these DEGs. The results showed that the GO terms associated with the DEGs were intermembrane lipid transfer, skeletal muscle thin filament assembly, protein secretion, and the cellular amino acid biosynthetic process (Fig. 2D). In addition, the shared and unique DEGs at each time point were presented in the Venn diagram (Fig. 2C), which revealed 46 linked genes being altered upon the ORFV infection. Across the three time points, 18 shared DEGs were significantly upregulated and were therefore targeted for subsequent functional analyses. The *KCNE4* gene, associated with the ion channels, was among the top 10 upregulated host genes (*ACTC1*, *DDX4*, *GRHL3*, *HMGA2*, *ITGA7*, *KCNH7*, *KCNE4*, *LRP2*, *OLFM1*, and *SEMA6A*) and was then hypothesized to play a role in the ORFV replication. The transcription level of *KCNE4* was examined by the RT-qPCR assay and it was found to have also increased significantly in the ORFV-infected STICs from 9 to 48 hpi (Fig. 2E).

Impacts of knockdown of the upregulated genes on ORFV replication

Considering the upregulation of these host genes in the ORFV-infected STICs, we aimed to investigate whether

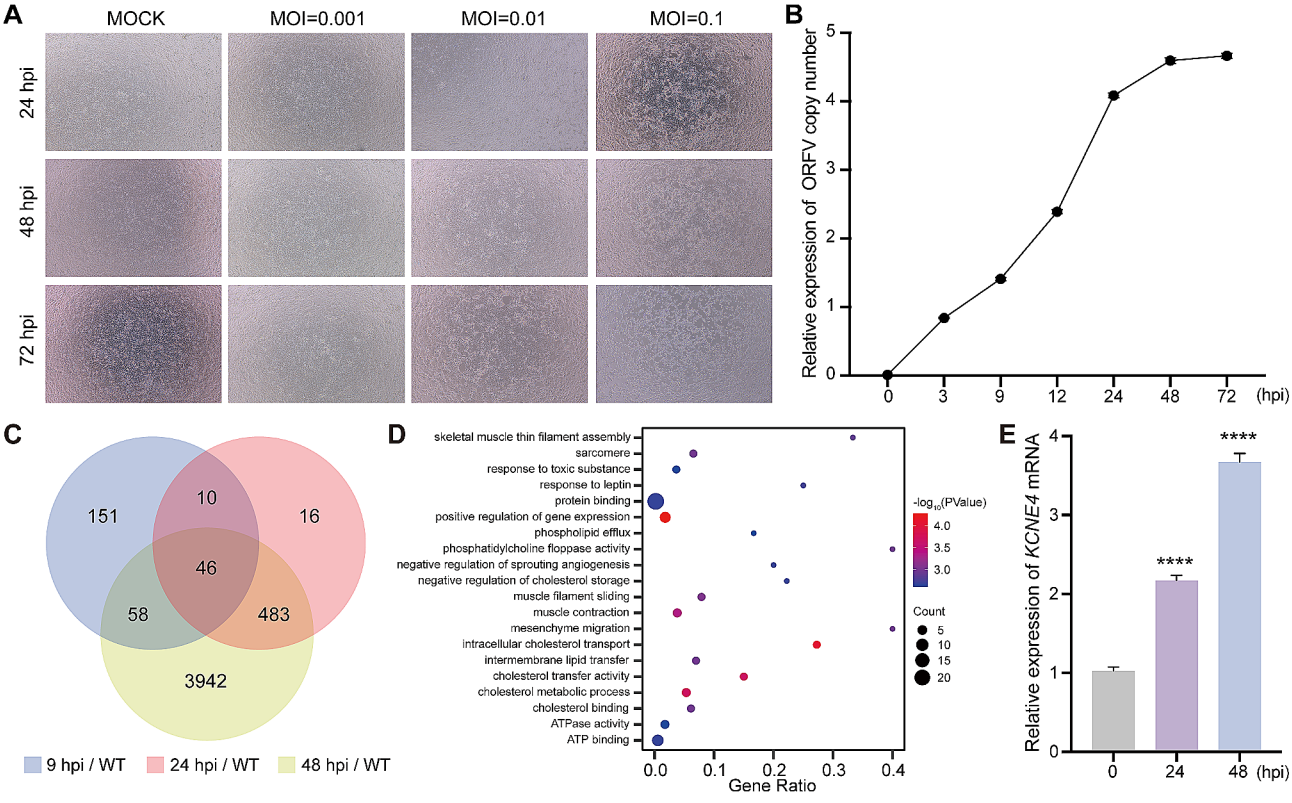

Fig. 2 Experimental design and data analysis for RNA-seq. **A** Growth of ORFV in STICs. Morphological changes of STICs at different time points (24, 48, and 72 hpi) and MOIs (0.1, 0.01, and 0.001) after infection with ORFV. **B** One-step growth curve of ORFV infection in STICs. STICs were infected with ORFV at an MOI of 0.1, and infected cells were collected at 3, 9, 12, 24, 48, and 72 hpi. The copy number of the virus was measured by an RT-qPCR assay. **C** Venn diagram of DEGs between WT and ORFV-infected cells. The blue, red, and yellow circles represent the DEGs at 9, 24, and 48 hpi, respectively. **D** GO functional enrichment analysis of DEGs between WT and ORFV-infected cells. **E** RT-qPCR validation for the expression level of the *KCNE4* gene after the ORFV infection

these genes are crucial during the ORFV lifecycle. The STICs were transfected with different siRNAs and then infected with ORFV at an MOI of 0.1. An RT-qPCR assay was performed to determine the inhibitory effect of gene-specific siRNAs. The transcriptions of these genes in the siRNA transfected and ORFV-infected STICs were found to be attenuated at 48 h post-transfection (Fig. 3A). To quantify the effect of siRNAs on viral replication, the copy number of ORFV genome was determined at 48 hpi. Compared with wild-type (WT) STICs, the transcription levels of the ORFV genome in the *KCNE4*, *KCNH7*, *ITGA7*, and *GRHL3* siRNA knockdown STICs were found to be significantly reduced. However, there was no difference in the copy number of ORFV genome between the *ACTC1*, *DDX4*, *HMGA2*, *LRP2*, *OLFM1*, and *SEMA6A*siRNA knockdown and WT STICs (Fig. 3B). Specifically, the *KCNE4* siRNA knockdown showed the most significant effect on the ORFV suppression.

Ion channels are a class of proteins that form ion-selective channels on the cell membrane, which play important roles in maintaining the homeostasis between the intracellular and extracellular compartments and regulating cell signaling and functions. The relationship between ion channels and viral invasion is a complex and interesting area of research that has not been fully clarified yet. Different types of ion channels may play specific roles in particular viral infection processes [15, 16]. Considering the importance of ion homeostasis during viral infection, we chose the *KCNE4* gene for subsequent analyses.

KCNE4 is a critical host factor for the ORFV infection

Similarly, ORFV can cause significant cytopathy in a variety of cell types such as HeLa cells, a human cancer cell line [17]. To demonstrate whether *KCNE4* could regulate the ORFV infection in human cells, we generated two clonal *KCNE4* KO HeLa cell lines through the CRISPR/Cas9 gene-editing system. Sanger sequencing results confirmed that the *KCNE4*-KO cell lines 1 and 2 contained 5- and 2-nucleotide deletions, respectively (Fig. 4A). Western blotting analysis showed that KCNE4 expression was reduced in the *KCNE4*-KO HeLa cells (Fig. 4B). In addition, there was no difference in cell viability between the *KCNE4*-KO and WT cells using the Cell Counting Kit-8 (CCK8) assay (Fig. 4C). Subsequently, we used an RT-qPCR assay to quantify the viral DNA from the ORFV-infected *KCNE4*-KO and WT cells. Given that the Hela cells are more susceptible to ORFV than the STICs, we chose to use a lower dose of ORFV to infect the *KCNE4*-KO Hela cells. The copy number of ORFV was significantly decreased in the *KCNE4*-KO cells after the infection at an MOI of 0.01 (Fig. 4D). Fluorescence and CPE assays revealed that knocking *KCNE4* out inhibited the ORFV transcription at 24 hpi (Fig. 4E and F). Similarly, the CCK8 assay showed a higher cell viability in the ORFV-infected *KCNE4*-KO Hela cells than in the WT Hela cells (Fig. 4G), indicating that knocking *KCNE4* out has a significant inhibitory effect on the ORFV infection. We then quantified the viral DNA from the ORFV-infected *KCNE4*-KO and WT HeLa cells by the RT-qPCR assay. Our results showed that the copy number of ORFV was significantly decreased in the *KCNE4*-KO HeLa cells at 12, 24, and 36 hpi (Fig. 4H). Consistent with the previous results, the fluorescence assay revealed that the number of ORFV-GFP in the *KCNE4*-KO HeLa cells was reduced at MOIs of 0.05, 0.1, 0.2, and 0.5 (Fig. 4I). Furthermore, the *KCNE4*-KO HeLa cells possessed diminished levels of ORFV-GFP at 12, 24, and 36 hpi (Fig. 4J). In addition, the *KCNE4*-KO and WT HeLa cells were

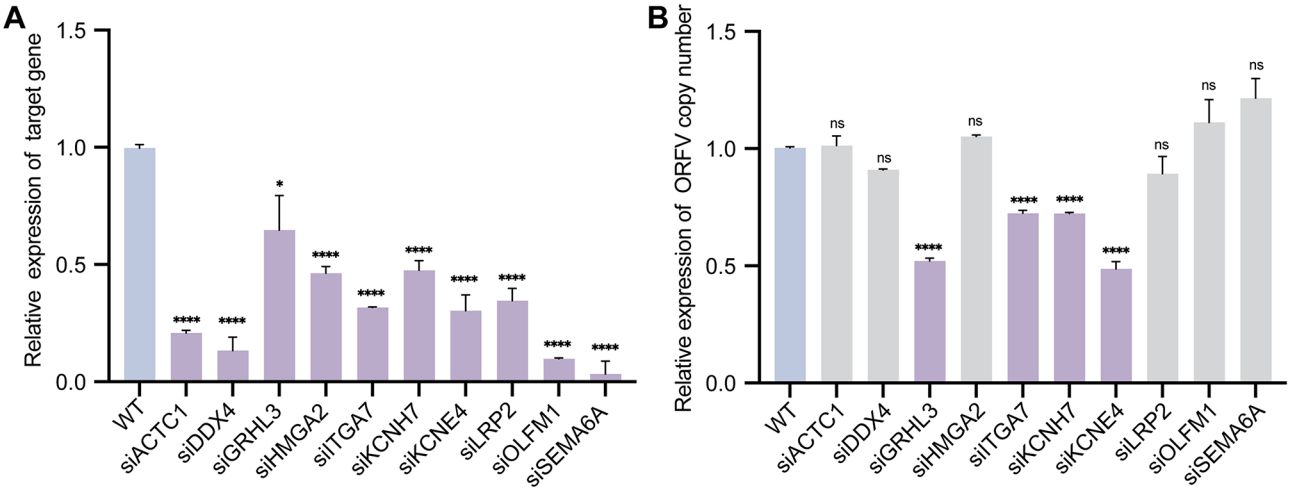

Fig. 3 Detection of the effect of the ten candidate genes by siRNA assay. **A** The mRNA level of the ten genes (*ACTC1*, *DDX4*, *GRHL3*, *HMGA2*, *ITGA7*, *KCNH7*, *KCNE4*, *LRP2*, *OLFM1*, and *SEMA6A*) in siRNA knockdown or negative control siRNA transfected STICs was quantified by RT-qPCR at 48 h post-transfection. **B** Relative expression of the ORFV copy number in the siRNA knockdown groups. STICs transfected with different siRNAs were infected with ORFV (MOI = 0.1). At the indicated time points, ORFV-infected cellular samples were collected and determined. ns: not significant, * $P < 0.05$, **** $P < 0.0001$

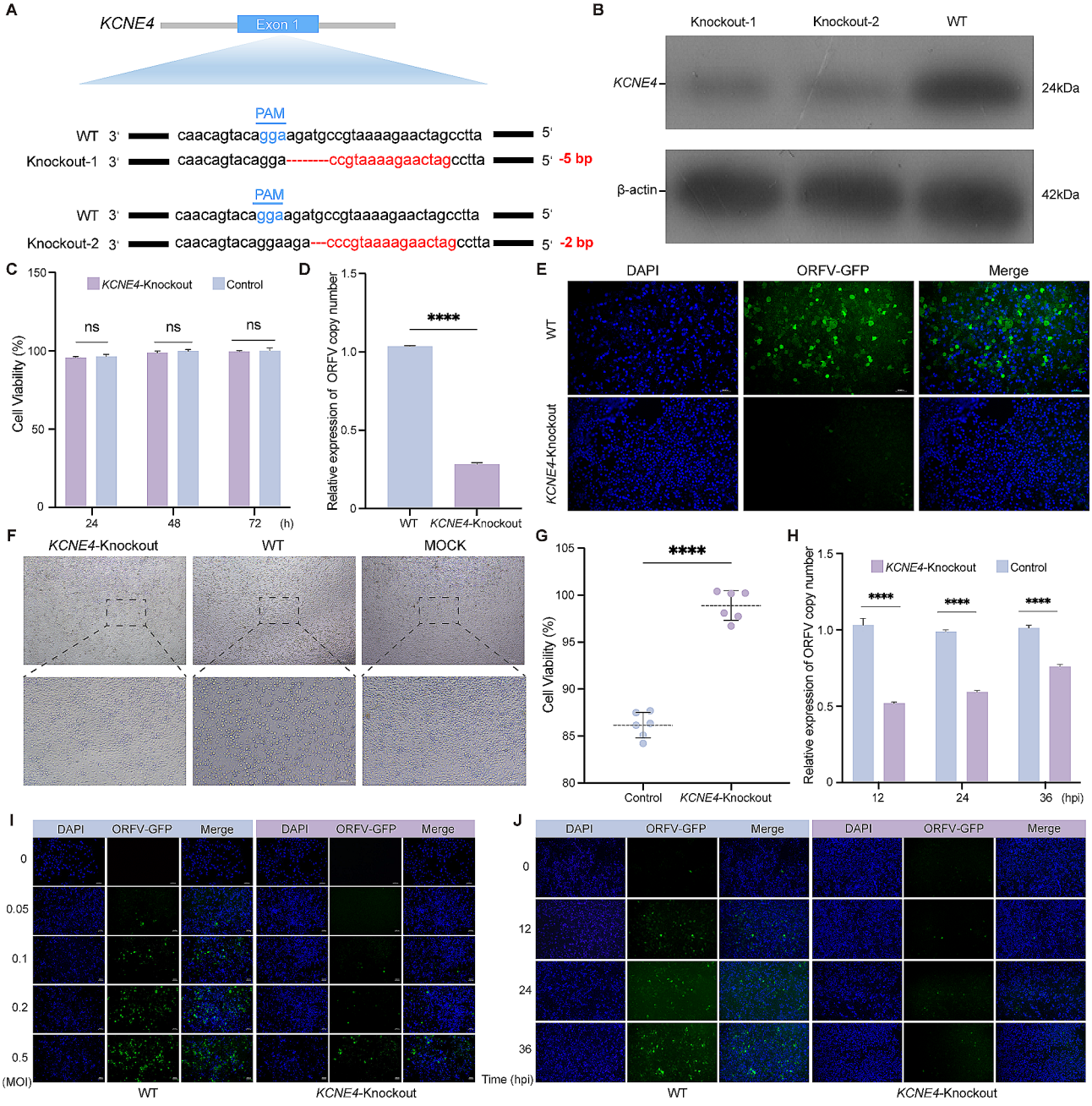

Fig. 4 *KCNE4* is a host factor required for ORFV infection in HeLa cells. **A** Alignment of the nucleic acid sequences of clonal knockout cells of *KCNE4* with the WT cells. sgRNA-targeting sites are highlighted in red. The red characters "-" indicate the deleted bases in the knockout cells. PAM sites are indicated in blue letters. **B** The knockout of *KCNE4* in HeLa cells was confirmed by Western blot. **C** The viability of *KCNE4*-KO and control cells was assessed using the CCK8 assay. **D** and **E***KCNE4*-KO and WT cells were infected with ORFV (MOI = 0.01) at 24 h, and cells were harvested for RT-qPCR and fluorescence assays, respectively. **F** ORFV-induced CPE in WT and *KCNE4*-KO cells infected with ORFV at an MOI of 0.01. Dotted frames indicate CPE induced by ORFV infection. **G** Assessment of cell viability in WT and *KCNE4*-KO cells after ORFV infection. **H***KCNE4*-KO and control cells were infected with ORFV (MOI = 0.01) at 12, 24, and 36 h, and ORFV DNA levels were determined by RT-qPCR. **I** and **J***KCNE4*-KO and WT cells were infected with ORFV-GFP at different MOIs (0.05, 0.1, 0.2, and 0.5), and a fluorescence assay was used to detect the ORFV-GFP expression at 12, 24, and 36 hpi. Scale bar, 200 μm. ns: not significant, **** $P < 0.0001$

infected with ORFV-GFP at MOIs of 0.02, 0.05, 0.1, and 0.2 for 24 h or 48 h. The level of fluorescence ratio was detected by fluorescence-activated cell sorting (FACS). We found that knocking *KCNE4* out from the HeLa cells inhibited the infection of ORFV-GFP (Fig. 5A-D). Taken together, different assays showed that the amount of ORFV in the *KCNE4*-KO HeLa cells was lower than the WT HeLa cells, indicating *KCNE4* to be a critical host factor for the ORFV infection.

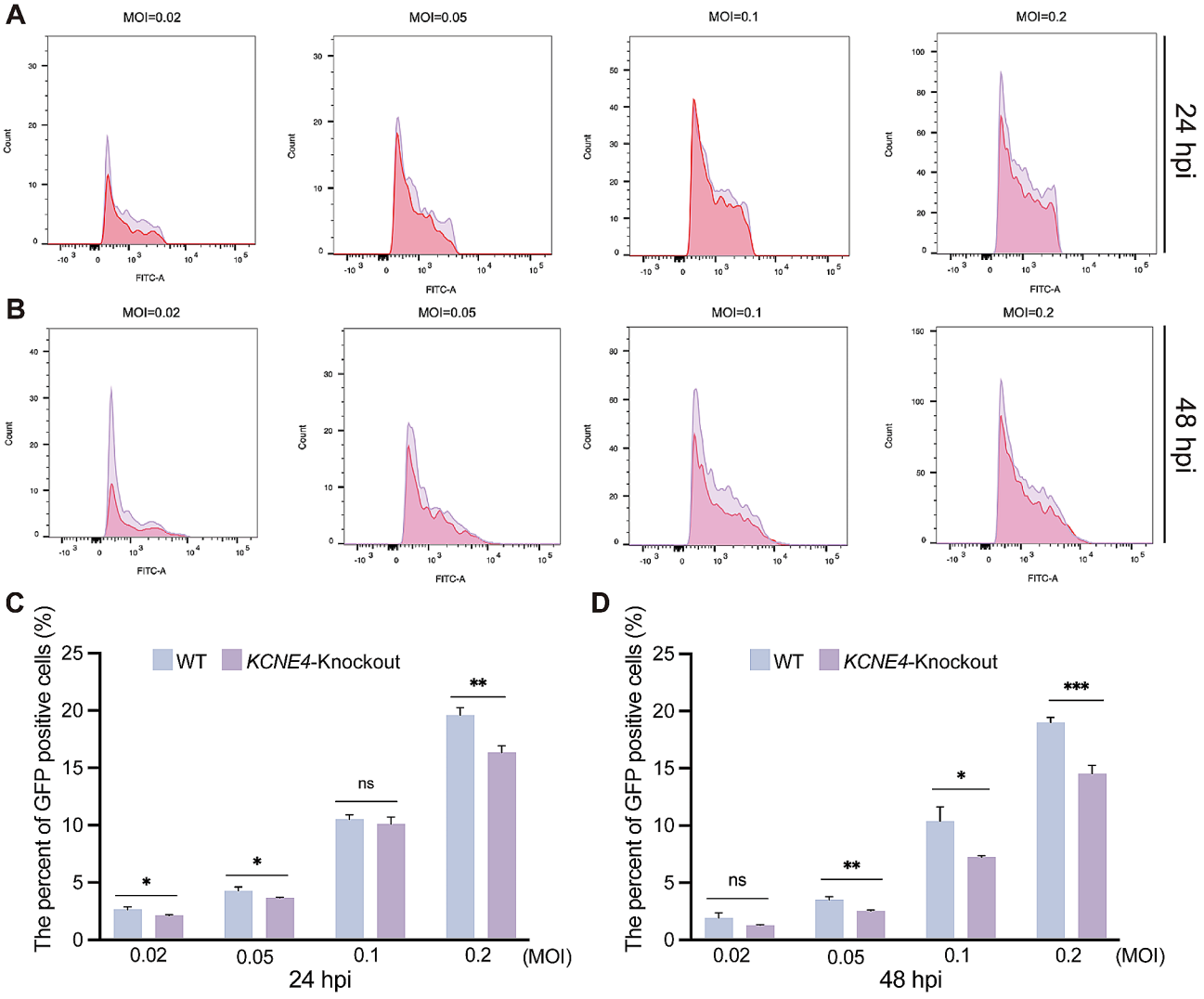

Fig. 5 *KCNE4* is a host gene essential for the ORFV infection. **A** and **B***KCNE4*-KO and WT cells were infected with ORFV-GFP at different MOIs (0.02, 0.05, 0.1, and 0.2) for 24–48 h. An FACS assay was used to detect ORFV-GFP expression. **C** and **D** The level of fluorescence ratio was analyzed by the GraphPad software

Knocking *KCNE4* out inhibits the entry of ORFV into the HeLa cells

Ion channels can affect the steps of viral entry, replication, and release, thereby affecting the infection efficiency and pathogenicity of the virus [18]. Given the above-mentioned results suggested *KCNE4* to be important in the ORFV infection, we sought to determine the stage of life cycle at which the ORFV infection is affected by *KCNE4*. The *KCNE4*-KO and WT HeLa cells were infected with ORFV and tested under different conditions. The attachment and internalization assays showed that *KCNE4* knockout suppressed ORFV entry into the Hela cells (Fig. 6). Subsequently, we assessed the impact of the *KCNE4* knockout on viral replication and release. We found that the amount of ORFV DNA was lower in the *KCNE4*-KO than the WT HeLa cells, indicating that *KCNE4* does play a role in the ORFV infection (Fig. 6). Overall, knocking *KCNE4* out from the HeLa cells reduced the ORFV attachment, internalization, replication, and release. Thus, these results indicate that *KCNE4* may intricately regulate gene expression to support the ORFV entry into the affected cells.

Effects of small-molecule antagonists on the ORFV infection

KCNE4 is one of the subunits of voltage-gated potassium ion channels, which can interact with KCNQ1 channels to form KCNQ1/KCNE4 ion channel complexes and participate in intracellular signal transduction. To examine whether K^+ channel inhibitors could affect the ORFV infection, we evaluated the effect of two inhibitors such as quinidine and fluoxetine on the ORFV infection in the

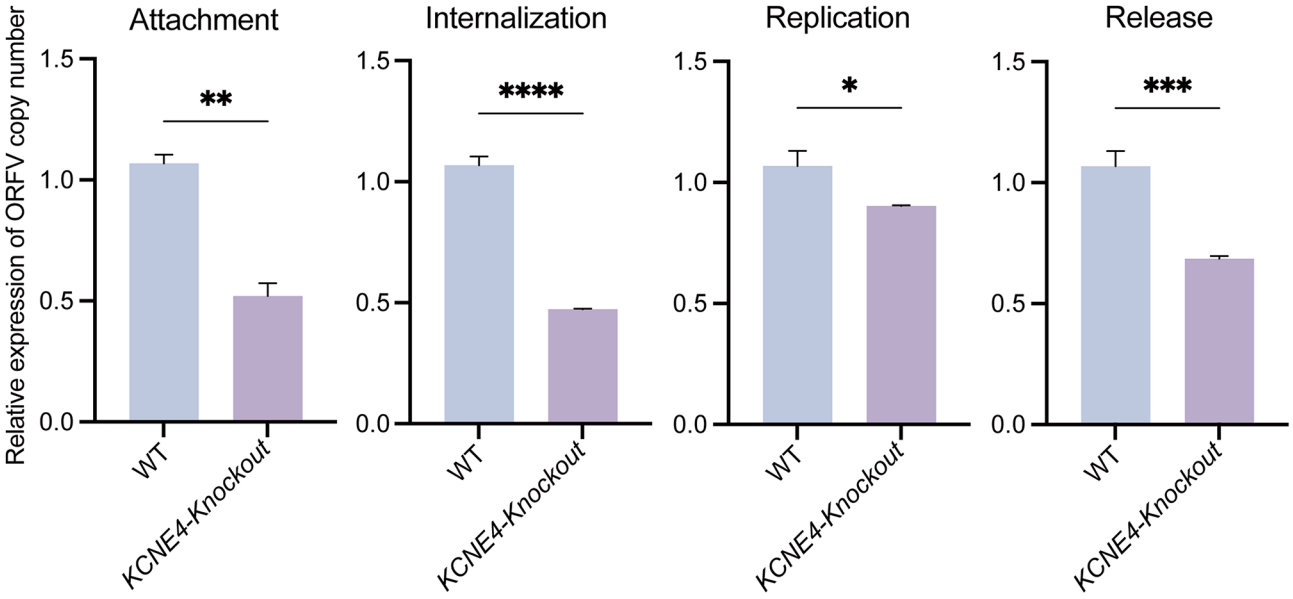

Fig. 6 Knockout of *KCNE4* inhibits the ORFV entry. *KCNE4*-KO and WT cells were infected with ORFV at 4 °C for 1 h and then harvested. An RT-qPCR assay was used to assess virion attachment at the cell surface. *KCNE4*-KO and WT cells were infected with ORFV for 1 h and then incubated at 37 °C for 2 h to allow the virus to get internalized. Cells were harvested, and viral internalization activity was assessed by an RT-qPCR assay. *KCNE4*-KO and WT cells were infected with ORFV, and then the cells were incubated at 37 °C for 5 h to allow the virus to replicate. The amount of viral DNA was detected by an RT-qPCR assay. *KCNE4*-KO and WT cells were infected with ORFV (MOI = 0.05) and incubated at 4 °C for 1 h. The cells were washed three times with PBS at 12 hpi and were cultured at 37 °C for another 2 h. The amount of viral DNA was detected by an RT-qPCR assay

STICs and HeLa cells. Cell proliferation was not affected after the treatment with certain concentrations of inhibitors, as determined by the CCK8 assay (Fig. 7A and D). Next, we analyzed the viability of STICs and HeLa cells treated with quinidine and fluoxetine. The results showed that the cell viability was higher in the inhibitor-treated groups than in the control groups after the ORFV infection (Fig. 7E and H). Subsequently, we assessed the impact of inhibitors on STICs and HeLa cells by fluorescence microscopy assay. The infection capacity of ORFV was significantly inhibited at different concentrations of quinidine and fluoxetine in STICs and HeLa cells (Fig. 7I and L). Taken together, these results revealed that targeted inhibition of *KCNE4* by quinidine and fluoxetine significantly suppressed the ORFV infection, implying that *KCNE4* was essential for the ORFV infection.

Discussion

Orf is a zoonotic disease induced by ORFV. ORFV could cause pustular lesions, and the morbidity rate may approach 90%, which poses a serious threat to human health and the economic loss of the livestock industry worldwide [19, 20]. However, there are few studies regarding the interaction between the ORFV infection and host cells. Thus, we performed an RNA-seq assay to explore ORFV-host interactions, providing a significant reference for the control and prevention of ORFV.

In this study, the proliferation of STICs infected with ORFV was investigated for the first time. We found that STICs were susceptible to the ORFV infection by microscopic observation and the RT-qPCR assay. For the purpose of identifying genes involved in the ORFV infection, we used RNA-seq to identify DEGs from the ORFV-infected STICs. GO enrichment analysis demonstrated that DEGs were mainly present in ion transport, intermembrane lipid transfer, and protein secretion. We then chose the ten shared DEGs at each time point (9, 24, and 48 hpi) for subsequent analysis. Our results showed that the ORFV infection was significantly inhibited in the *KCNE4*, *KCNH7*, *ITGA7*, and *GRHL3* siRNA knockdown cells, suggesting that the four candidate genes have antiviral effects on STICs. It is noteworthy that knockdown of *KCNE4* expression exhibited the most significant viral inhibition. Therefore, we mainly aimed to investigate the role of *KCNE4* in the ORFV infection.

KCNE4 is the 4th member of the KCNE Kv channel regulatory subunit family, which encodes a single-spanning membrane protein [21]. Previous studies have shown that *KCNE4* is a key regulator in leukocytes and physically interacts with the Kv1.3 channel, altering its trafficking and electrophysiological properties [22]. Currently, there has been increasing evidence that *KCNE4* is associated with the disease of atrial fibrillation [23]. In the present study, our findings revealed that *KCNE4* is an essential host factor that could reduce ORFV viral DNA production. We further found that down-regulation of the *KCNE4* expression significantly reduced the ORFV

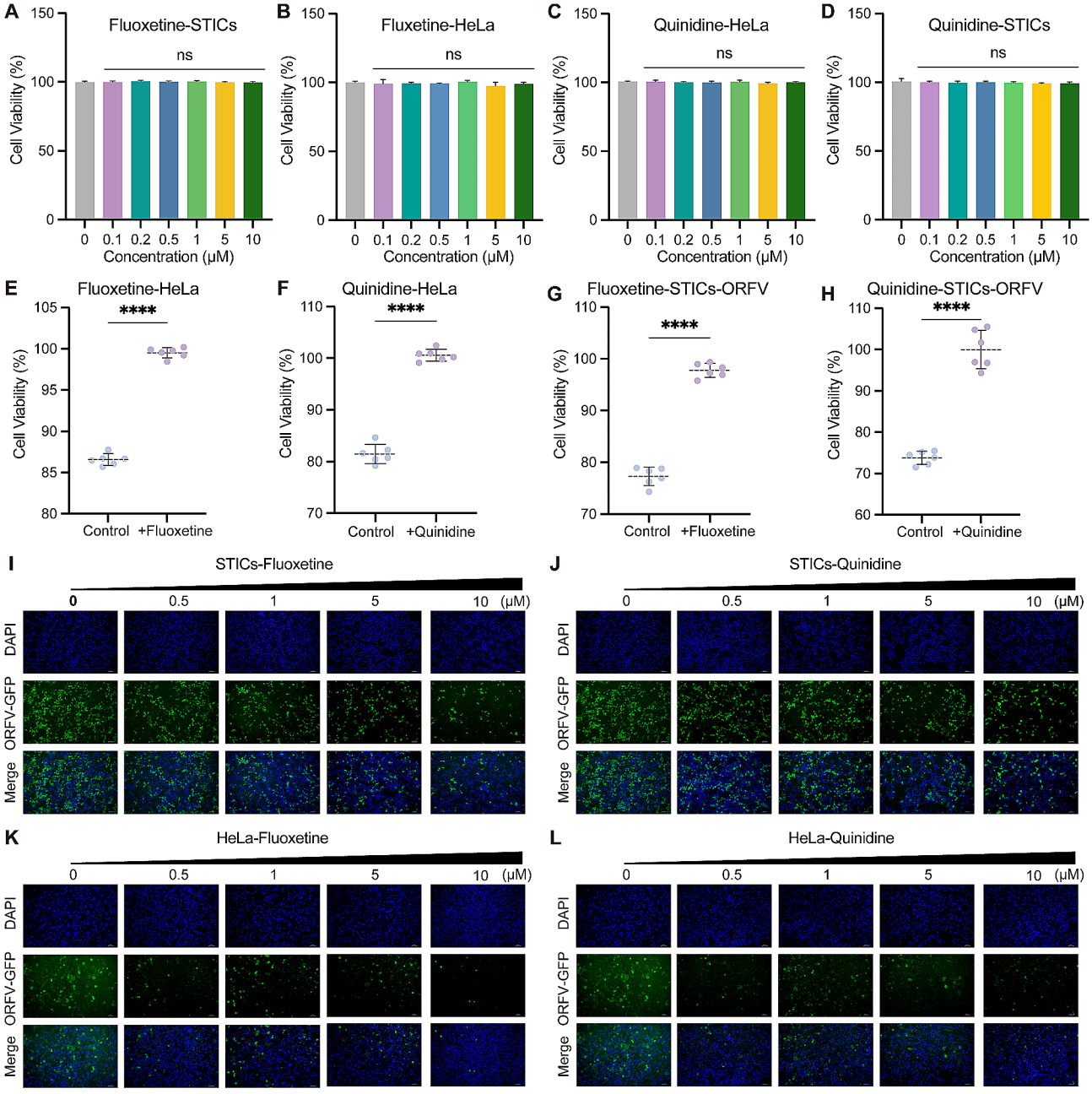

Fig. 7 Small molecules inhibit the ORFV infection. **A**-**D** STICs and HeLa cells were incubated with different concentrations (0.1, 0.2, 0.5, 1, 5, and 10 μM) of quinidine and fluoxetine, respectively. Cell viability was tested by the CCK8 assay. **E**-**H** The effects of quinidine and fluoxetine in ORFV-infected cells. Cell viability was determined by the CCK8 assay. **I**-**L** STICs and HeLa cells were incubated in advance with different concentrations of quinidine and fluoxetine, and the cells were treated with ORFV. A fluorescence microscopy assay was performed to test the effects of inhibitors on the ORFV infection. Scale bar, 200 μm. ns: not significant, **** $P < 0.0001$

entry, suggesting that *KCNE4* is a critical host factor for promoting the ORFV infection.

Quinidine is known as a classic I_A antiarrhythmic drug that can nonspecifically inhibit Na^+ influx and K^+ outflow [24]. A previous study has shown that it reduces seizure frequency [25]. Fluoxetine might affect the gut viral community [26]. Both quinidine and fluoxetine are inhibitors of the K^+ potassium channel. Here, we found that quinidine and fluoxetine could significantly inhibit the ORFV infection, suggesting that the inhibitors may have an antiviral effect against ORFV. Based on these analyses, we hypothesize that *KCNE4* may regulate the function of the K^+ potassium channel to influence the ORFV infection. However, the exact regulation remains unclear, and further studies are needed to explore the detailed mechanisms.

Several limitations would be dissected in future research, including (i) the need to evaluate the ORFV susceptibility in human and other cell lines and (ii) the need to further investigate the mechanisms between ORFV receptor genes and host cells. Taken together, our study provides an in-depth insight into the ORFV infection, which may help in the development of antiviral drugs and disease prevention.

Conclusions

Our study demonstrated for the first time that *KCNE4* plays an important role in the ORFV infection. *KCNE4* knockout downregulated the expression of ORFV, resulting in impaired virus entry. In addition, small-molecule inhibitors targeting the K^+ potassium channel were able to inhibit ORFV infection. Taken together, these findings enrich our understanding of the interaction mechanism between *KCNE4* and the ORFV infection.

Materials and methods

Cell culture

STICs and HeLa cells were purchased from the Cell Bank of the Chinese Academy of Sciences (Shanghai, China). The cells were cultured in Dulbecco's modified eagle medium (DMEM, Gibco, USA) supplemented with 10% fetal bovine serum (FBS, BI, Israel) and 1% penicillin/streptomycin (Beyotime, China). Cells were maintained at 37 °C with 5% CO_2.

Virus infection

The wild virus LY/2012/China strain of ORFV was provided by the Lanzhou Veterinary Research Institute, the Chinese Academy of Agricultural Sciences (Lanzhou, China), and the titer of the virus stock used was $10^{-2.5}$/100 μL. The recombinant ORFV-GFP was derived from the ORFV strain with the CBP gene replaced by the GFP expression cassette from the U6-GFP plasmid (a gift from ShanghaiTech University). After cells were infected with ORFV at different MOIs (the ratio of virus to target cells), the cells were incubated at 37 °C for 1 h, and the unbound virus was removed by washing the cells three times with phosphate-buffered saline (PBS). The cells were cultured at 37 °C for 72 h.

RNA-seq

STICs were infected with ORFV at an MOI of 1, and cellular samples were collected at 9, 24, and 48 hpi. Total RNA was extracted from the infected STICs using TRIzol Reagent (Invitrogen, USA). The transcriptome sequencing and analysis were conducted by BGI-DNBSEQ (BGI, China). A corrected P value of <0.05 and an absolute fold change ($|\log_2 FC|$) of >2 were set as the thresholds for significantly differential expression.

Small interfering RNA (RNAi) assay

RNAi negative control and targeting siRNAs for ten candidate genes (*ACTC1*, *DDX4*, *GRHL3*, *HMGA2*, *ITGA7*, *KCNH7*, *KCNE4*, *LRP2*, *OLFM1*, and *SEMA6A*) were commercially synthesized from Gene Pharma (Shanghai, China). A total of 0.1×10^6 cells per well were seeded in a 12-well plate. When STICs were grown to 80% confluence, 40 pmol siRNAs per well were transfected into STICs using Lipo8000 Transfection Reagent (Beyotime, China) according to the manufacturer's instructions. The knockdown efficiency of the candidate genes was determined by RT-qPCR at 48 hpi. Each assay was performed in triplicate. Primer sequences are shown in Additional file 1: Table S1.

Construction of KO HeLa cell lines for candidate genes

We designed single guide RNAs (sgRNAs) to knockout candidate genes in HeLa cells and cloned them into the pGL3-U6-sgRNA-GFP vector (a gift from Huang Xingxu's lab, ShanghaiTech University, China) using *Bsa*I (NEB, China). For transfection, 0.5 μg of sgRNA plasmid and 2 μg of Cas9 plasmid were transfected using Lipo8000 Transfection Reagent (Beyotime, China). After 48 h of transfection, cells with green fluorescent protein expression were identified by FACS. The GFP-positive cells were then seeded into 96-well plates. Wells containing single-cell clones were expanded and used for genomic DNA extraction (CWBIO, China) and PCR amplification. Genomic DNA from the cells was extracted using the Universal Genomic DNA Kit (CWBIO, China). The knockout efficiency was confirmed by Sanger sequencing of the PCR products and Western blotting assessments of the protein expression of target genes. Primer sequences are shown in Additional file 1: Table S2.

Cell viability assay

WT and KO HeLa cells were planted into 96-well plates with 2×10^3 cells/well. Cell viability was determined every 24 h with the CCK8 Kit (Beyotime, China). For the inhibitor assay, STICs and HeLa cells were planted into 96-well plates with 2×10^3 cells/well. On the next day, the medium was replaced with DMEM/10% FBS supplemented with various concentrations of certain quinidine or fluoxetine. The absorbance at 450 nm was detected with a microplate reader.

RT-qPCR

Viral DNA was extracted using the TIANamp Virus DNA Kit (TIANGEN, China). Total RNA from the cell genome was extracted using the RNA Easy Fast Cell Kit (TIANGEN, China). The complementary DNA (cDNA) was obtained by RT-qPCR using ReverTra Ace qPCR RT Master Mix (TOYOBO, Japan). The RT-qPCR assay

was performed in triplicate using SYBR qPCR Master Mix (Vazyme, China) in a Light Cycle Roche 480 II RT-qPCR system (Roche, Switzerland). The relative expression level was calculated using the $2^{-\Delta\Delta Ct}$ method. Primer sequences are shown in Additional file 1: Table S3.

Flow cytometry

WT and *KCNE4*-KO HeLa cells were seeded onto 24-well plates 24 h prior to infection. Cells were infected with ORFV-GFP (MOIs=0.02, 0.05, 0.1, and 0.2) for 24–48 h and digested with trypsin-EDTA (Gibco, USA). Then, the cells were collected by centrifugation at 1,000 *rpm* for 5 min and resuspended in PBS. The percentage of GFP-positive cells was measured by flow cytometry. All data were acquired and analyzed using FlowJo.

Treatment of inhibitors

Quinidine (MCE, HY-B1751) and fluoxetine (MCE, HY-B0102) were dissolved in dimethyl sulfoxide (DMSO) at a stock concentration of 1 mM and stored at -80 °C. STICs and HeLa cells were incubated with the specified concentration of inhibitors for 2 h and then infected with ORFV at an MOI of 0.01. Then, the cells were prepared for cell viability and fluorescence assays at 24 hpi.

Western blotting

Cells were collected and lysed with the RIPA lysis buffer (Beyotime, China). Lysates were mixed with 5× SDS-PAGE sample loading buffer (Beyotime, China) and heated at 95 °C for 10 min. Then, proteins were subjected to 12.5% SDS-PAGE and transferred onto a polyvinylidene fluoride (PVDF) membrane. The PVDF membrane was blocked by nonfat dry milk for 1 h. Next, the PVDF membrane was incubated overnight at 4 °C with specific primary antibodies, including KCNE4 (Abcam, USA) and β-actin (Abcam, USA). Subsequently, goat anti-rabbit IgG (H+L) secondary antibody (Thermo, USA) was applied at 1:5,000 dilutions and incubated at 37 °C for 1 h. Finally, the proteins were detected with ECL Prime Western Blotting Detection Reagents (Beyotime, China).

Virus attachment, internalization, replication, and release assays

To test the effect of *KCNE4* on ORFV attachment to the cell surface, we cultured WT and *KCNE4*-KO cells in 24-well plates and treated them with ORFV (MOI=10) at 4 °C for 1 h. After being washed with ice-cold PBS, the viral DNA was extracted from infected cells and evaluated by an RT-qPCR assay. To determine the effect of *KCNE4* on ORFV internalization, the cells were seeded onto 24-well plates and incubated with 10 MOI ORFV at 4 °C for 1 h. Next, the cells were washed three times with PBS and incubated at 37 °C for 2 h. Afterward, the cells were harvested, and virus infection was detected by RT-qPCR. The ORFV replication assay was conducted by infecting WT and *KCNE4*-KO cells with ORFV (MOI=1) at 37 °C for 1 h and washed three times with PBS. Then, the cells were incubated at 37 °C for 5 h. The DNA expression level of ORFV was determined by RT-qPCR. To examine the effect of *KCNE4* on ORFV release, the cells were infected with ORFV (MOI=0.05) and incubated at 4 °C for 1 h. The cells were washed three times with cold PBS at 12 hpi and were cultured at 37 °C for another 2 h. Finally, viral DNA in the supernatant was detected by RT-qPCR.

Statistical analysis

Statistical analysis was performed using the Student's two-tailed unpaired *t*-test or an analysis of variance (ANOVA) with GraphPad Prism 9.0 software. Data are expressed as the means ± SD. ns: not significant, * $P<0.05$, ** $P<0.01$, *** $P<0.001$, and **** $P<0.0001$.

Supplementary Information

The online version contains supplementary material available at https://doi.org/10.1186/s12985-024-02454-3.

Supplementary Material 1

Acknowledgements

Not applicable.

Author contributions

Authors' contributionsConceptualization: Xiaolong Wang, Jianlin Han, Wenxin Zheng.Funding acquisition: Xiaolong Wang, Wenxin Zheng.Investigation: Jiayuan Sun, Yige Ding.Resources: Keshan Zhang, Weiwei Wu.Validation: Jiayuan Sun, Yige Ding.Visualization: Qian Zhou, Peter Kalds.Writing-original draft: Jiayuan Sun, Yinghui Wei.Writing-review & editing: Peter Kalds, Jianlin Han, Xiaolong Wang.

Funding

This work was supported by the Sci-Tech Innovation 2030 Key Program (2023ZD0405104), the National Key Research and Development Program of China (2023YFF1000900), the National Natural Science Foundation of China (U23A20228 and 32272848), and the China Agricultural Research System (CARS-39-03).

Data availability

No datasets were generated or analysed during the current study.

Declarations

Ethics approval and consent to participate

All methods and experimentations were performed in accordance with the relevant guidelines and regulations of the Animal Care and Use Committee of Northwest A&F University, China.

Consent for publication

All authors have read and approved the manuscript.

Competing interests

The authors declare no competing interests.

Received: 28 April 2024 / Accepted: 31 July 2024
Published online: 08 August 2024

References

1. Bergqvist C, Kurban M, Abbas O. Orf virus infection. Rev Med Virol. 2017;27(4). https://doi.org/10.1002/rmv.1932.
2. Demiraslan H, Dinc G, Doganay M. An overwiev of ORF Virus Infection in humans and animals. Recent Pat Antiinfect Drug Discov. 2017;12(1):21–30.
3. Spyrou V, Valiakos G. Orf virus infection in sheep or goats. Vet Microbiol. 2015;181(1–2):178–82.
4. Zhou Y, Gao F, Lv L, Wang S, He W, Lan Y, Li Z, Lu H, Song D, Guan J, Zhao K. Host factor cyclophilin B affects Orf virus replication by interacting with viral ORF058 protein. Vet Microbiol. 2021;258:109099.
5. Long M, Wang Y, Chen D, Wang Y, Wang R, Gong D, Luo S. Identification of host cellular proteins LAGE3 and IGFBP6 that interact with Orf virus protein ORFV024. Gene. 2018;661:60–7.
6. Vallejo-Gracia A, Sastre D, Colomer-Molera M, Solé L, Navarro-Pérez M, Capera J, Roig SR, Pedrós-Gámez O, Estadella I, Szilágyi O, Panyi G, Hajdú P, Felipe A. KCNE4-dependent functional consequences of Kv1.3-related leukocyte physiology. Sci Rep. 2021;11(1):14632.
7. Roux B. Ion channels and ion selectivity. Essays Biochem. 2017;61(2):201–9.
8. Fujioka Y, Nishide S, Ose T, Suzuki T, Kato I, Fukuhara H, Ohba Y. A Sialylated voltage-dependent Ca^{2+} Channel binds Hemagglutinin and mediates Influenza A Virus Entry into mammalian cells. Cell Host Microbe. 2018;23(6):809–e8185.
9. Hover S, Foster B, Fontana J, Kohl A, Goldstein S, Barr JN, Mankouri J. Bunyavirus requirement for endosomal K + reveals new roles of cellular ion channels during infection. PLoS Pathog. 2018;14(1):e1006845.
10. Müller KH, Kakkola L, Nagaraj AS, Cheltsov AV, Anastasina M, Kainov DE. Emerging cellular targets for influenza antiviral agents. Trends Pharmacol Sci. 2012;33(2):89–99.
11. Panyi G, Varga Z, Gáspár R. Ion channels and lymphocyte activation. Immunol Lett. 2004;92(1–2):55–66.
12. Solé L, Roura-Ferrer M, Pérez-Verdaguer M, Oliveras A, Calvo M, Fernández-Fernández JM, Felipe A. KCNE4 suppresses Kv1.3 currents by modulating trafficking, surface expression and channel gating. J Cell Sci. 2009;122(Pt 20):3738–48.
13. Solé L, Roig SR, Vallejo-Gracia A, Serrano-Albarrás A, Martínez-Mármol R, Tamkun MM, Felipe A. The C-terminal domain of Kv1.3 regulates functional interactions with the KCNE4 subunit. J Cell Sci. 2016;129(22):4265–77.
14. Solé L, Roig SR, Sastre D, Vallejo-Gracia A, Serrano-Albarrás A, Ferrer-Montiel A, Felipe A. The calmodulin-binding tetraleucine motif of KCNE4 is responsible for association with Kv1.3. FASEB J. 2019;33(7):8263–79.
15. Charlton FW, Pearson HM, Hover S, Lippiat JD, Fontana J, Barr JN, Mankouri J. Ion channels as therapeutic targets for viral infections: further discoveries and future perspectives. Viruses. 2020;12(8):844.
16. Pietschmann T. Clinically approved Ion Channel inhibitors close Gates for Hepatitis C Virus and Open doors for Drug Repurposing in infectious viral diseases. J Virol. 2017;91(2):e01914–16.
17. Harvey R, McCaughan C, Wise LM, Mercer AA, Fleming S. B. Orf virus inhibits interferon stimulated gene expression and modulates the JAK/STAT signalling pathway. Virus Res. 2015;208:180–8.
18. Lang Y, Li F, Liu Q, et al. The Kv1.3 ion channel acts as a host factor restricting viral entry. FASEB J. 2021;35(2):e20995.
19. Bukar AM, Jesse FFA, Abdullah CAC, et al. Immunomodulatory strategies for Parapoxvirus: current status and future approaches for the development of vaccines against Orf Virus infection. Vaccines (Basel). 2021;9(11):1341.
20. Wang R, Wang Y, Liu F, Luo S. Orf virus: a promising new therapeutic agent. Rev Med Virol. 2019;29(1):e2013.
21. Tian K, Tao Z, Chen Y, et al. KCNE4 expression is correlated with the pathological characteristics of colorectal cancer patients and associated with the radioresistance of cancer cells. Pathol Res Pract. 2023;241:154234.
22. Navarro-Pérez M, Estadella I, Benavente-Garcia A, et al. The phosphorylation of Kv1.3: a modulatory mechanism for a multifunctional Ion Channel. Cancers (Basel). 2023;15(10):2716.
23. Mao T, Miao HJ, Xu GJ, et al. Zhonghua Xin xue guan bing za zhi. 2013;41(11):916–21.
24. Liu R, Sun L, Wang Y, Wang Q, Wu J. New use for an old drug: quinidine in KCNT1-related epilepsy therapy. Neurol Sci. 2023;44(4):1201–6.
25. Bearden D, Strong A, Ehnot J, DiGiovine M, Dlugos D, Goldberg EM. Targeted treatment of migrating partial seizures of infancy with quinidine. Ann Neurol. 2014;76(3):457–61.
26. Li J, Qu W, Hu C, Liu Z, Yan H. Antidepressants Amitriptyline, fluoxetine, and traditional Chinese medicine Xiaoyaosan caused alterations in gut DNA virome composition and function in rats exposed chronic unpredictable mild stress. Front Microbiol. 2023;14:1132403.

Publisher's Note